The Astronomical Journal, 152:25 (11pp), 2016 July doi:10.3847/0004-6256/152/1/25

THE UV-BRIGHT QUASAR SURVEY (UVQS): DR1

TalaWanda R. Monroe[1], J. Xavier Prochaska[2], Nicolas Tejos[2], Gabor Worseck[3], Joseph F. Hennawi[3], Tobias Schmidt[3], Jason Tumlinson[1], and Yue Shen[4]
[1] Space Telescope Science Institute, Baltimore, MD, 21218, USA
[2] Department of Astronomy and Astrophysics, UCO/Lick Observatory, University of California, 1156 High Street, Santa Cruz, CA 95064, USA
[3] Max-Planck-Institut für Astronomie, Königstuhl 17, D-69115 Heidelberg, Germany
[4] Department of Astronomy and National Center for Supercomputing Applications, University of Illinois at Urbana-Champaign, Urbana, IL 61801, USA
Received 2015 December 11; accepted 2016 February 3; published 2016 July 1

ABSTRACT

We present the first data release (DR1) from our UV-bright Quasar Survey for new $z \sim 1$ active galactic nuclei (AGNs) across the sky. Using simple *GALEX* UV and *WISE* near-IR color selection criteria, we generated a list of 1450 primary candidates with FUV < 18.5 mag. We obtained discovery spectra, primarily on 3 m-class telescopes, for 1040 of these candidates and confirmed 86% as AGNs, with redshifts generally at $z > 0.5$. Including a small set of observed secondary candidates, we report the discovery of 217 AGNs with FUV < 18 mag that previously had no reported spectroscopic redshift. These are excellent potential targets for UV spectroscopy before the end of the *Hubble Space Telescope* mission. The main data products are publicly available through the Mikulski Archive for Space Telescopes.

Key words: intergalactic medium – quasars: general

Supporting material: machine-readable tables

1. INTRODUCTION

Presently, the only efficient means of studying the diffuse gas surrounding galaxies (a.k.a. halo gas or the circumgalactic medium, CGM) and in between galaxies (a.k.a. the intergalactic medium, IGM) is through absorption-line spectroscopy of luminous, background quasars (e.g., Tripp et al. 2008; Tumlinson et al. 2013; Tejos et al. 2014). Furthermore, because the principal transitions to diagnose gas lie at far-ultraviolet (FUV) wavelengths ($\lambda_{\rm rest} < 2000$ Å), for $z < 1$ studies, one requires UV spectrometers on space-borne facilities. Currently, and for the foreseeable future, the *Hubble Space Telescope* (*HST*) affords the only opportunity for such research, primarily with the Cosmic Origins Spectrograph (COS). Given the modest aperture of *HST*, these observations are generally restricted to the brightest FUV quasars on the sky.

High-quality, FUV spectroscopy of $z \sim 1$ quasars has enabled several unique experiments to study the CGM and IGM of the universe over the past ∼10 Gyr. These include: (1) the survey of highly ionized gas via the Ne VIII$\lambda\lambda$770, 780 doublet and/or broad H I Lyα systems that may trace the elusive warm-hot ionized medium (e.g., Lehner et al. 2007; Meiring et al. 2013; Tejos et al. 2016); (2) the search for signatures of galactic and active galactic nucleus (AGN) feedback (e.g., Tripp et al. 2011); (3) the measurements of enrichment in galactic halos and optically thick gas (e.g., Lehner et al. 2013; Werk et al. 2013, 2014); and (4) revealing the structure of the cosmic web and its correlation to the large-scale structures traced by galaxies (e.g., Tejos et al. 2014). While each of these programs has had a scientific impact, they are limited by sample variance.

An efficient way to increase the volumes surveyed is to focus on those bright UV QSOs that maximize the redshift path covered, i.e., those with $z_{\rm em} \gtrsim 1$. To date, only a small number of $z \sim 1$ quasars have been observed with *HST*, primarily corresponding to the set of sources with very high FUV flux. These have been drawn from historical, large-area surveys for AGNs (e.g., the Palomar-Green Bright Quasar Survey and the Hamburg/ESO survey) and more recently the Northern Galactic pole footprint of the Sloan Digital Sky Survey (SDSS). Cross-matching the quasar sample of Flesch (2015) against the point-source catalog of the *GALEX* survey, one recovers ≈140 sources with $z > 0.6$ and FUV < 18 mag (fewer than 50 at $z > 1$). These are preferentially located within the SDSS footprint, which has extensively surveyed the Northern galactic pole for quasars (e.g., Schneider et al. 2010). Given that *HST* may observe nearly any position on the sky, we are motivated to perform an all-sky search for new, FUV-bright quasars across the sky. Indeed, progress in this area demands the discovery of new FUV-bright quasars.

The principal goal of our survey is to provide the community with a nearly complete set of UV-bright AGNs before the termination of the *HST* mission. We recognized that the combination of two NASA imaging missions—*GALEX* and *WISE*—enables a modern, all-sky search for UV bright quasars. These must be spectroscopically confirmed, however, before subsequent *HST* observations. Given our interest in FUV-bright sources, this implies optically bright candidates that can be spectroscopically confirmed on 3 m-class telescopes. The following manuscript provides the first data release (DR1) from our UV-bright Quasar Survey (UVQS). The main data products are available at the Mikulski Archive for Space Telescopes.[5]

This paper is organized as follows. Section 2 describes the UVQS candidate selection, focused on detecting $z \sim 1$ quasars with FUV < 18 mag. The follow-up spectroscopy is discussed in Section 3 and the redshift analysis is described in Section 4. We present the primary results in Section 5. When relevant, we

[5] https://archive.stsci.edu/prepds/uvqs

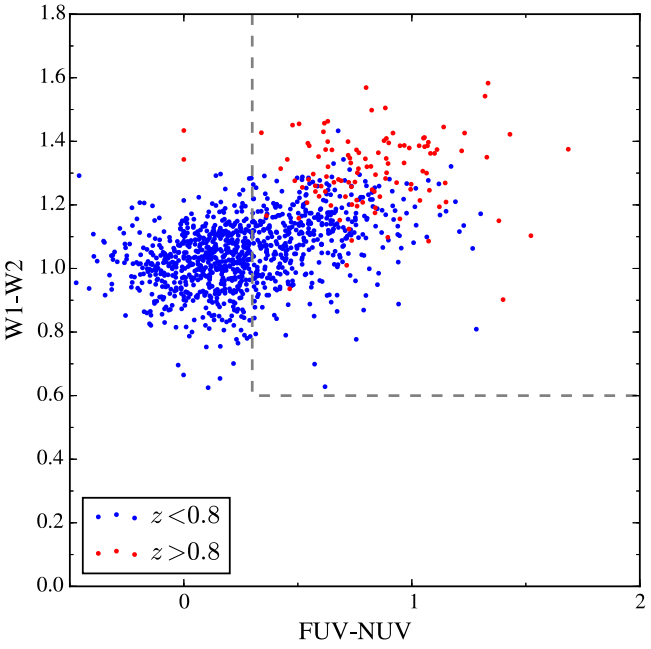

Figure 1. Color-color plot of *WISE* and *GALEX* photometry of the SDSS DR7 quasars (Schneider et al. 2010) that have an NUV flux <19 mag. It is evident that each has a $W1 - W2 > 0.6$ mag color, consistent with the Stern et al. (2012) selection criteria for AGNs. Furthermore, the $z > 0.8$ quasars exhibit redder FUV–NUV colors, which we hypothesize results from intervening Lyman limit opacity. The gray dashed lines at $W1 - W2 = 0.6$ mag and FUV–NUV = 0.3 mag indicate the color–color criteria adopted for our primary candidates (Table 1).

assume a ΛCDM cosmology with $h = 0.7$, $\Omega_m = 0.3$, and $\Omega_\Lambda = 0.7$.

2. THE UVQS CANDIDATES

With the explicit goal of discovering new FUV-bright quasars at $z \sim 1$ across the sky, we developed color–color criteria, leveraging the all-sky surveys of the *WISE* and *GALEX* missions to (i) isolate AGNs and (ii) maximize the probability that these AGNs lie at $z_{\rm em} \gtrsim 1$. For the first criterion, we followed the impressive results from the *WISE* team who demonstrated the clean separation of AGNs from stars, galaxies, and other astrophysical sources using *WISE* photometry (Stern et al. 2012). Specifically, Stern et al. (2012) showed that AGNs tend to exhibit $W1 - W2 > 0.4$ mag, with galaxies and stars having smaller values. Although this criterion may not capture all AGNs (e.g., Assef et al. 2010), we strongly expect that every UV-bright AGN satisfies the criterion. Indeed, we find that of the 1148 quasars at $z < 1.5$ from SDSS DR7 detected by *GALEX* (NUV < 19.0), all have $W1 - W2 > 0.625$ mag (Figure 1). The overwhelming majority of these have $z < 0.8$ (90%).

Figure 1 also shows the FUV–NUV colors of these quasars. These were measured from the "photoobjall" catalog of the GALEXGR6Plus7 context at MAST and improved, where possible, using the MIS catalog ("bcscat_mis" Bianchi et al. 2014). We see that the majority of $z < 0.8$ quasars have FUV–NUV < 0.3 mag (60%) and that nearly all of the $z > 0.8$ quasars have a redder FUV–NUV color. We believe that this "reddening" primarily results from the presence of one or more Lyman limit systems (LLSs) in the redshift interval $0.5 < z < 0.8$, whose continuum opacity reduces only the FUV flux. We infer that nearly every $z \sim 1$ quasar exhibits at least one intervening LLS[6] with $N_{\rm H\,I} > 10^{16.7}$ cm^{-2}.

With our photometric criteria established,

$$W1 - W2 > 0.6 \text{ mag} \quad (1)$$

$$\text{FUV–NUV} > 0.3 \text{ mag} \quad (2)$$

$$\text{FUV} < 18.5 \text{ mag}, \quad (3)$$

we cross-matched every source in the GALEXGR6Plus7 catalogs[7] satisfying these criteria against the AllWISE Source Catalog. To avoid selecting already known quasars given the beam sizes of *WISE* and *GALEX*, we then eliminated any sources that lay within 5″ of a UV-bright quasar from SDSS DR7. This generated a list of 1450 primary candidates (Table 1). We discovered, during our analysis, that this candidate list includes hundreds of previously cataloged sources from other surveys. This includes the SDSS-III survey which included *WISE*-selected quasar targets (Pâris et al. 2014). Their primary *WISE* criteria, however, precluded overlap with our sample. Given that several of these surveys have known examples of false redshift identifications or do not provide the discovery spectra, we maintained the list and re-observed many of the brighter sources (FUV < 18 mag). Figure 2 shows an all-sky summary of the UVQS candidates, separated by FUV flux. The exclusion of the Galactic plane is obvious and the lower incidence of sources in the SDSS footprint is notable.

In several of the observing runs, conditions were unexpectedly favorable and we exhausted the primary candidates at certain R.A. ranges. To fill the remaining observing time, we generated a secondary candidate list with one criterion modified: $-0.5 <$ FUV–NUV < 0.3. This would permit a much higher fraction of low-z AGNs, but may also yield a few sources at $z \sim 1$. This secondary set of candidates is provided in Table 2.

3. OBSERVATIONS AND DATA PROCESSING

We proceeded to obtain discovery-quality longslit spectra (i.e., low-dispersion, large wavelength coverage, modest signal-to-noise ratio (S/N) of our UVQS candidates in one calendar year. Our principal facilities were: (i) the dual Kast spectrometer on the 3 m Shane telescope at the Lick Observatory; (ii) the Boller & Chivens (BCS) spectrometer on the Irénée du Pont 100″ telescope at the Las Campanas Observatory; and (iii) the Calar Alto Faint Object Spectrograph on the CAHA 2.2 m telescope at the Calar Alto Observatory (CAHA). We acquired an additional ≈20 spectra on larger aperture telescopes (Keck/ESI, MMT/MBC, *Magellan*/MagE) during twilight or under poor observing conditions. Typical exposure times were limited to $\lesssim$200 s, with adjustments for fainter sources or sub-optimal observing conditions. Table 3 provides a list of the observed candidates.

[6] In standard IGM nomenclature, LLSs with $N_{\rm H\,I} < 10^{17.3}$ cm^{-2} are often referred to as partial LLS or pLLS.

[7] Our explicit cassjobs query for the AIS data was: select objid, ra, dec, fuv_mag as fuv, nuv_mag as nuv from photoobjall; where fuv_mag BETWEEN 12. and 18.5; and (fuv_mag-nuv_mag) BETWEEN −0.5 and 2.0; and fuv_mag > −999; and nuv_mag > −999. We then used the following for the MIS to improve the photometry: select objid, ra, dec, fuv_mag as fuv, nuv_mag as nuv from bcscat_mis; where fuv_mag BETWEEN 12. and 18.5; and (fuv_mag-nuv_mag) BETWEEN −0.5 and 2.0; and fuv_mag > −999; and nuv_mag > −999.

Table 1
UVQS DR1 Primary Candidates

Name	α_{J2000} (°)	δ_{J2000} (°)	*W1* (mag)	*W2* (mag)	FUV (mag)	NUV (mag)
UVQSJ000000.15–200427.7	0.00064	−20.07437	13.55	12.54	18.27	17.97
UVQSJ000002.92–350332.6	0.01218	−35.05905	12.69	11.55	17.61	17.31
UVQSJ000009.66–163441.5	0.04023	−16.57819	13.43	12.19	18.48	17.72
UVQSJ000037.52–752442.6	0.15633	−75.41184	11.69	10.63	17.81	17.45
UVQSJ000355.89–224122.4	0.98286	−22.68955	13.24	12.11	17.97	17.24
UVQSJ000503.70–391747.9	1.26542	−39.29664	12.26	11.12	17.82	17.23
UVQSJ000609.57–261140.6	1.53989	−26.19460	13.31	12.12	18.16	17.53
UVQSJ000613.29+321534.6	1.55537	32.25960	12.93	11.75	18.42	17.95
UVQSJ000717.70+421646.7	1.82374	42.27963	12.44	11.51	18.09	17.61
UVQSJ000741.01–635145.9	1.92085	−63.86274	12.65	11.45	17.96	17.41
UVQSJ000750.79+031733.1	1.96161	3.29253	12.98	11.58	17.80	17.01
UVQSJ000755.68+052818.8	1.98200	5.47189	13.12	11.73	18.07	17.29
UVQSJ000814.36+121201.4	2.05983	12.20039	13.64	12.49	18.20	17.73
UVQSJ000827.05–405126.6	2.11270	−40.85740	12.83	12.17	18.46	18.10
UVQSJ000856.77–235317.6	2.23655	−23.88821	13.00	11.73	18.32	16.89
UVQSJ001015.62–624045.2	2.56509	−62.67921	13.68	12.42	18.39	17.75
UVQSJ001121.73–200212.2	2.84055	−20.03671	13.10	11.81	18.42	17.53
UVQSJ001127.08–143314.3	2.86282	−14.55399	13.05	12.42	17.80	17.46
UVQSJ001155.61–240438.9	2.98169	−24.07747	13.16	12.02	18.24	17.16
UVQSJ001250.39–214704.9	3.20997	−21.78469	12.65	11.53	17.97	17.45
UVQSJ001444.03–223522.6	3.68344	−22.58961	13.16	11.77	18.39	17.34

(This table is available in its entirety in machine-readable form.)

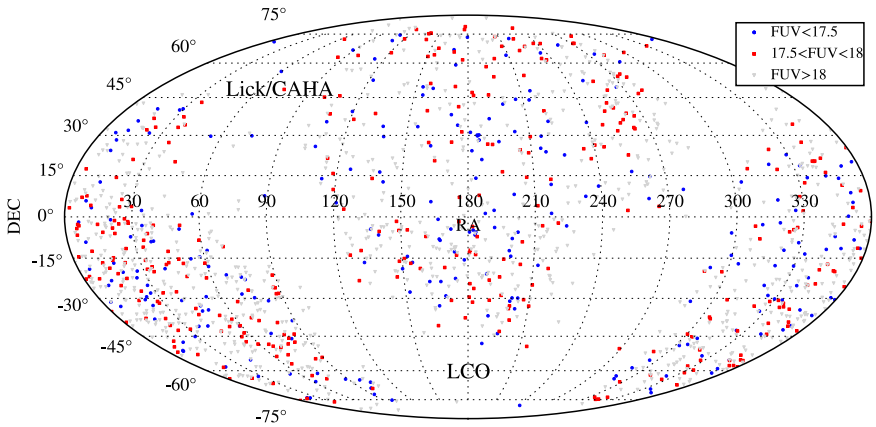

Figure 2. All-sky plot describing the spatial distribution of our primary candidates, coded by FUV flux. We have avoided the Galactic plane and also note that there are fewer targets toward the Northern Galactic pole (i.e., within the SDSS footprint).

The two-dimensional (2D) spectral images and calibration frames were reduced with custom software, primarily the LowRedux package[8] developed by J. Hennawi, X. Prochaska, and D. Schlegel. Briefly, the images were bias-subtracted, flat-fielded using quartz lamp spectral images, and wavelength-calibrated with arc-lamp exposures. Objects within the slit were automatically identified and optimally extracted to 1D spectra. These were fluxed after generating a sensitivity function from observations of spectrophotometric standard stars taken during each observing run. We did not carefully account for varying atmospheric conditions and we did not correct for slit-losses from variable seeing or atmospheric dispersion. Therefore, the reported fluxes are crude and not even especially accurate in a relative sense, particularly at the wavelength extrema. Although we occasionally obtained multiple exposures for a given source, these were not combined; the highest quality spectrum was analyzed. Upon visual inspection we assigned a spectral data quality number (SPEC_QUAL) to each spectrum. Our scale spans 0–5, in which 0 is poor, or unusable, and 5 is excellent. SPEC_QUAL values are a good proxy for S/N and are included in Table 3. Note that even spectra without spectral features may have a high SPEC_QUAL value.

The calibrated 1D spectra are published in DR1 and provided at https://archive.stsci.edu/prepds/uvqs. We also present a cut-out, optical image of each source taken from the SDSS or DSS surveys. Figure 3 shows representative spectra from the UVQ DR1 sample, including examples of a Galactic star, a low-z AGN, and a $z > 1$ quasar (PHL 1288). At the S/N of these spectra (each of which has a spectral quality of 4 or 5), redshift identification is straightforward. We note that ≈50% of our spectra have this data quality and another 40% have SPEC_QUAL = 3, which we consider sufficient for redshift analysis.

[8] http://www.ucolick.org/~xavier/LowRedux/

Table 2
UVQS DR1 Secondary Candidates

Name	α_{J2000} (°)	δ_{J2000} (°)	*W1* (mag)	*W2* (mag)	FUV (mag)	NUV (mag)
UVQSJ000007.85–633535.2	0.03271	−63.59311	13.25	12.32	18.06	17.77
UVQSJ000011.73+052317.4	0.04886	5.38818	11.90	10.88	18.37	18.30
UVQSJ000024.03–275153.5	0.10013	−27.86486	12.85	11.80	18.32	18.14
UVQSJ000024.42–124547.9	0.10173	−12.76331	11.08	10.08	15.82	15.78
UVQSJ000036.68–634123.7	0.15285	−63.68991	12.44	11.46	18.10	18.15
UVQSJ000053.51–443933.5	0.22297	−44.65930	12.56	11.81	17.95	17.95
UVQSJ000054.29+183021.4	0.22621	18.50594	13.26	12.18	16.65	16.47
UVQSJ000055.97+172338.9	0.23320	17.39414	13.13	12.09	17.71	17.83
UVQSJ000103.53–114725.9	0.26469	−11.79053	12.70	11.59	18.04	18.13
UVQSJ000115.89+051902.1	0.31621	5.31725	13.47	12.61	18.43	18.44
UVQSJ000118.99+172425.3	0.32913	17.40703	12.86	11.88	18.48	18.33
UVQSJ000128.58–320842.1	0.36908	−32.14502	13.17	12.05	18.30	18.03
UVQSJ000146.09–765714.3	0.44203	−76.95396	11.01	10.23	17.05	16.88
UVQSJ000150.56+111647.3	0.46068	11.27981	11.68	10.73	17.27	17.12
UVQSJ000200.53–073907.5	0.50220	−7.65209	14.11	13.01	18.19	18.13
UVQSJ000210.06+171558.2	0.54193	17.26616	15.50	14.85	18.46	18.16
UVQSJ000211.74–342623.7	0.54890	−34.43992	13.19	12.16	18.22	18.09
UVQSJ000226.43+032106.9	0.61011	3.35191	10.76	10.13	16.39	16.14
UVQSJ000253.61–260346.4	0.72338	−26.06289	13.21	12.07	17.97	17.84
UVQSJ000316.84–275627.0	0.82017	−27.94084	12.53	11.60	17.76	17.64
UVQSJ000327.65+200919.5	0.86523	20.15542	13.30	12.27	18.34	18.06

(This table is available in its entirety in machine-readable form.)

Table 3
UVQS DR1 Observations

Name	Observatory	Instrument	Date	SPEC_QUAL[a]
UVQSJ000000.15–200427.7	LCO	BCS	2014 Aug	3
UVQSJ000009.65–163441.4	LCO	BCS	2014 Aug	3
UVQSJ000503.70–391747.9	LCO	BCS	2014 Aug	3
UVQSJ000609.57–261140.5	LCO	BCS	2014 Aug	3
UVQSJ000613.28+321534.5	Lick	Kast	2015 Jan	2
UVQSJ000717.69+421646.6	Lick	Kast	2015 Jan	4
UVQSJ000741.00–635145.8	LCO	BCS	2014 Aug	3
UVQSJ000750.78+031733.1	LCO	BCS	2014 Aug	4
UVQSJ000755.67+052818.8	LCO	BCS	2014 Aug	3
UVQSJ000814.35+121201.3	Lick	Kast	2015 Jan	1
UVQSJ000856.77–235317.5	LCO	BCS	2014 Aug	4
UVQSJ001015.62–624045.1	LCO	BCS	2014 Aug	3
UVQSJ001121.73–200212.1	LCO	BCS	2014 Aug	3
UVQSJ001155.60–240438.8	LCO	BCS	2014 Aug	4
UVQSJ001444.02–223522.6	LCO	BCS	2014 Aug	3
UVQSJ001521.62–385419.1	LCO	BCS	2014 Aug	3
UVQSJ001529.53–360535.3	LCO	BCS	2014 Aug	3
UVQSJ001637.90–054424.8	Lick	Kast	2015 Jan	3
UVQSJ001641.88–312656.6	*Magellan*	MagE	2014 Jul	5
UVQSJ001653.66–530932.6	LCO	BCS	2014 Aug	3
UVQSJ001655.68+054822.9	LCO	BCS	2014 Aug	3

Note.
[a] Spectral quality: 0—Too poor for analysis; 5—Excellent.

(This table is available in its entirety in machine-readable form.)

4. REDSHIFT ANALYSIS

To estimate the redshift of each source, we employed modified versions of the SDSS IDLUTILS software designed to measure quasar redshifts in that survey (Schneider et al. 2010). Specifically, we smoothed the quasar eigenspectra of SDSS (file: spEigenQSO-55732.fits) to match the spectral resolution from each of our instruments and then fit these

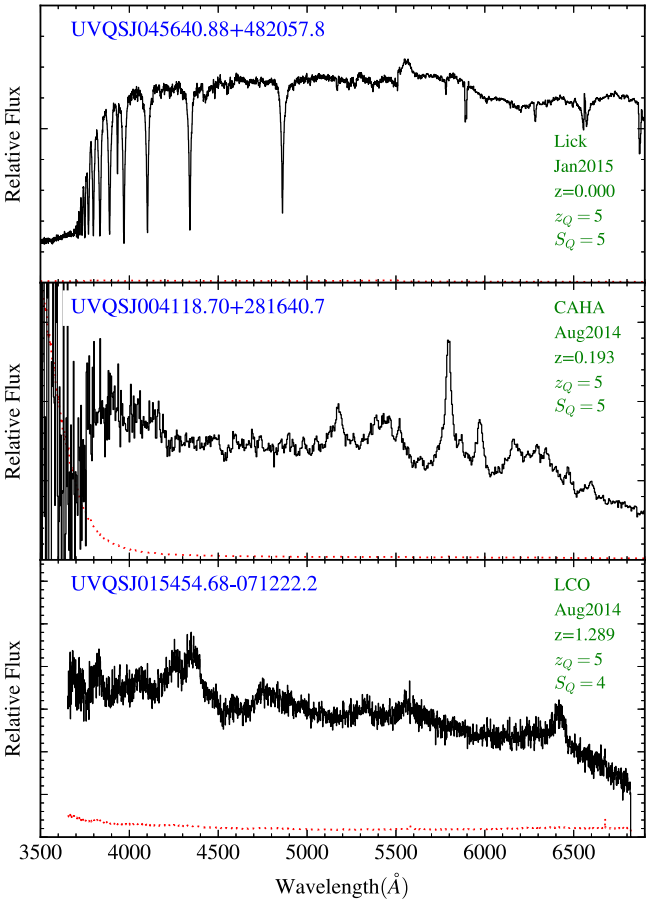

Figure 3. Characteristic spectra of the UVQS DR1 data release. From top to bottom, we show examples of a Galactic star, a low-z AGN, and a $z > 1$ quasar. The red dotted lines show an estimate of the 1σ uncertainties.

eigenspectra to each spectrum, minimizing χ^2. The algorithms provide the best redshift, the model eigenvalues, and a statistical estimate of the redshift uncertainty $\sigma(z)$.

All of the 1D spectra were visually inspected by at least two authors using a custom GUI to assess the spectra quality. In parallel, we assessed the redshift measurement by examining the best fit to the data. As necessary (~30% of the cases), we performed our own estimation of the redshift by identifying standard AGN emission features (primarily Mg II and Hβ). We then refitted templates to the data using a restricted redshift interval. We assessed the final redshift estimate based on the data quality and the number of spectral features identified and assigned a numerical quality assessment Z_QUAL with a scale of 0 (no estimate possible) to 5 (excellent estimate). Typically, sources with one prominent emission feature with a high-confidence assignment were given Z_QUAL = 3. The majority of these are AGNs with $z \approx 0.5$ where the Mg II emission line occurs at $\lambda \approx 4000$ Å and the expected Hβ emission feature falls redward of our spectral coverage. Many of these spectra show weak Balmer emission (e.g., Hγ) and/or continuum features that give high confidence to the reported redshift. Furthermore, associating the detected feature with another emission line (e.g., C III]) is strongly disfavored due to the non-detection of other, expected features. When multiple emission features were detected at a common redshift, the quality of the redshift determinations is given a 4 or 5 on our scale. From the total candidate list (Tables 1 and 2), we measured a high-quality redshift (Z_QUAL $\geqslant$ 3) for 1121 unique sources.

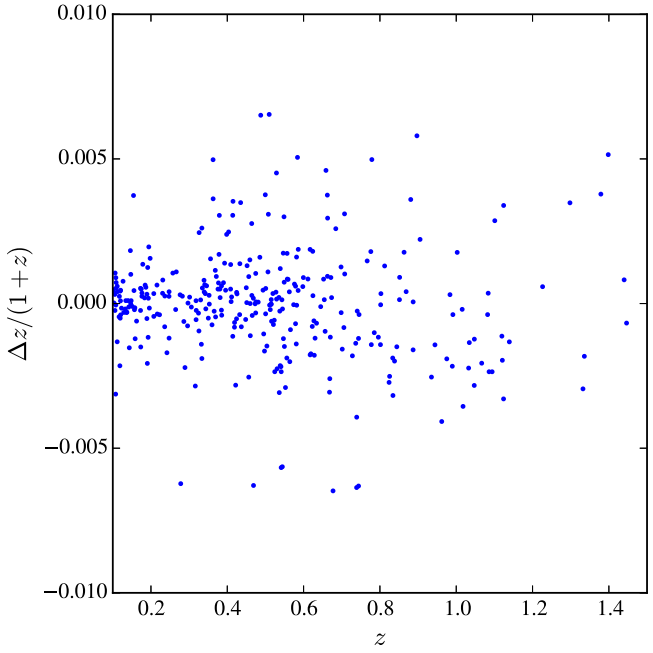

Figure 4. Redshift differences between measurements from our UVQS spectroscopy and the values listed in the MILLIQUAS catalog. With the exception of a few outliers (described in the text), there is very good agreement (rms $\approx$ 0.002).

In the following we assume that every source with a recessional velocity $v_r \equiv zc < 500$ km s^{-1} is "Galactic," which we associate with the Galaxy and members of the Local Group. This included sources where the eigenspectra fits were poor yet a low v_r was indisputable (e.g., stars). Many of these were assigned $z = 0$ exactly. The remainder of UVQS sources are assumed to be extragalactic AGNs, and are presented in Table 4. We caution, however, that we have neither assessed the relative line-fluxes of these sources nor assessed the widths of emission lines to confirm AGN activity. On the other hand, every source has a $W1 - W2$ color in excess of 0.6 mag and therefore has a high probability of containing an AGN.[9] Furthermore, nearly all of these sources exhibit at least one broad emission feature that is indicative of an AGN.

For the redshift uncertainty of the extragalactic sources, we have adopted the larger of $\sigma(z)$ derived from the eigenspectra analysis and 0.003. The latter value represents a systematic uncertainty from our procedure and also allows for the uncertainties in deriving a systemic redshift from broad, far-UV emission lines (e.g., Richards et al. 2002). We note, however, that many of the sources with $z < 0.5$ exhibit [O III] emission that may provide a smaller redshift uncertainty.

To assess the quality of our redshift estimates, we have compared our values against the Million Quasar Catalog (MILLIQUAS; v4.5) compiled by Flesch (2015). We restricted the MILLIQUAS sample to sources with spectroscopic redshifts (TYPE = A or Q) and we cross-matched in R.A., decl. to a 5 arcsec radius. In our first assessment, we noted two sources with a very large redshift difference: UVQSJ000856.77–235317.5 and UVQSJ231148.97+353541.4. In each of our spectra, there is a single broad emission feature. For UVQSJ000856.77–235317.5, we had

[9] The obvious exception will be chance superpositions of two sources, which we estimate to be a very rare occurrence (<1%).

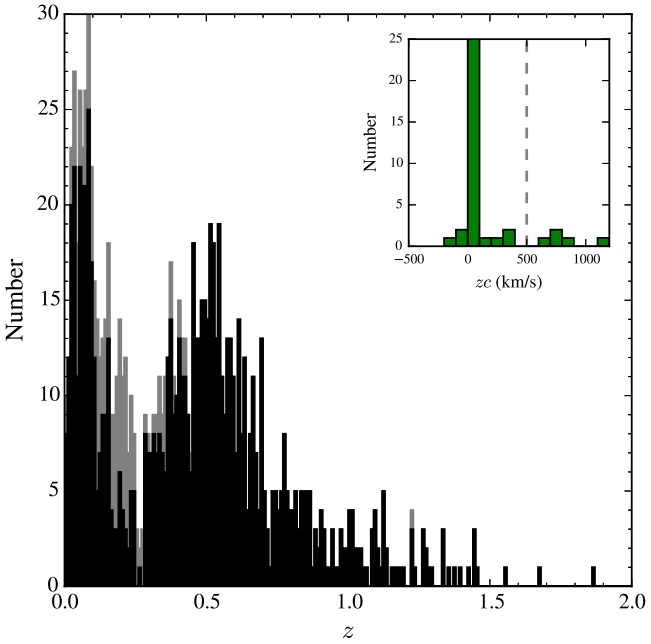

Figure 5. Redshift histogram of all sources with Z_QUAL > 3 from the UVQ DR1 database. The primary candidates (black) are dominated by sources at $z > 0.4$ with a tail to nearly 2. In contrast, the secondary candidates (gray) are confined to $z < 0.5$ and are primarily at $z < 0.2$. These results further highlight the efficacy of our primary FUV–NUV criterion. The inset shows the recession velocities $v_r \equiv zc$ of sources with $v_r \approx 0$ km s^{-1}. We associate all sources with $v_r < 500$ km s^{-1} with the Local Group.

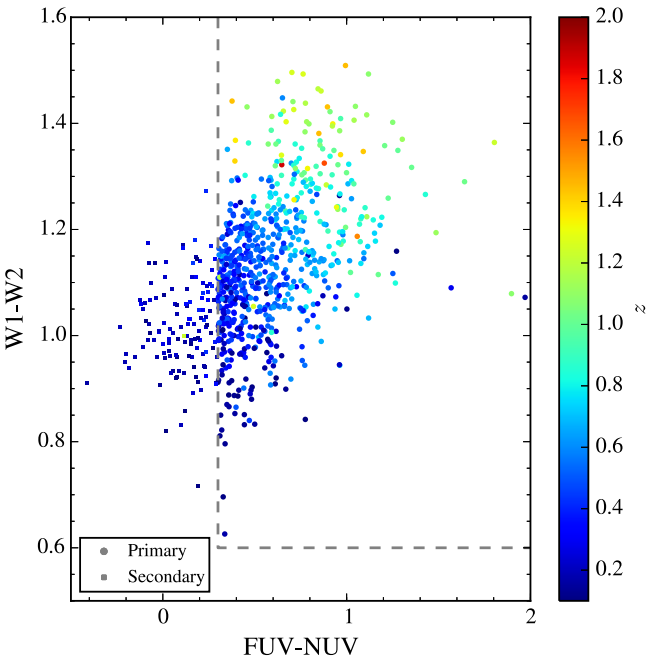

Figure 6. Near-IR and UV colors of the UVQS DR1 AGNs from the primary (circles) and secondary (square) candidate lists. The AGNs show a systematic reddening of both colors with increasing redshift. The near-IR evolution is related to a *k*-correction, whereas we believe the UV evolution is dominated by an increasing average opacity to Lyman limit absorption.

initially identified the feature as C III] emission, yet corresponding C IV emission is not apparent. Therefore, we revised our evaluation to mark this line as Mg II emission and revised the redshift accordingly; it is consistent with the previously cataloged value. The other source is a similar case with the

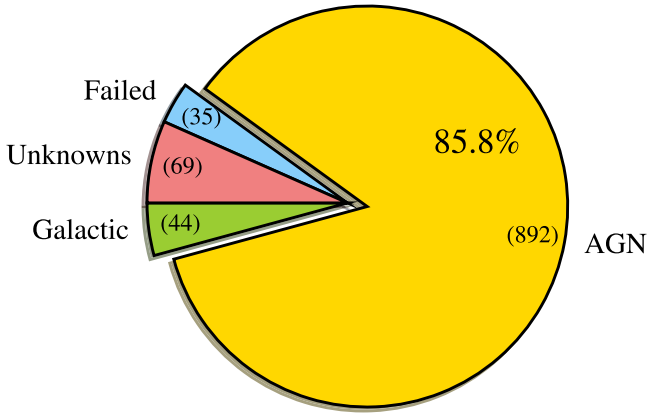

Figure 7. Distribution of the source classifications for the primary candidates observed in UVQS DR1. The color–color criteria yielded a very high incidence of AGNs. Formally, the reported rate for AGNs (86%) is a lower limit, as we expect many of the failed and unknown sources are also AGNs.

line identifications reversed; we have specified the line to be Mg II emission. If the line were C III], as previously assumed, the quasar should have shown Mg II emission. Given that there are also weak features at the expected wavelengths of H γ and H β for our preferred redshift, we have maintained our estimate for the source redshift.

Figure 4 summarizes the differences in redshifts $\delta z \equiv \Delta z/(1+z)$ between our measurements and those previously reported in the literature. Ignoring the anomalous cases described above, we measure an rms of 0.002 for the 191 sources with $z > 0.1$.

We present a histogram of the sources with well-constrained redshifts (Z_QUAL $\geqslant 3$) in Figure 5. For the primary candidates (black), there are two distributions at $z \approx 0.1$ and $z \approx 0.5$. The former are low-z AGNs, while the other set contains our desired targets. These exhibit a tail of redshifts to nearly $z = 2$. As expected, the sources drawn from our secondary list of candidates (gray) are primarily at $z < 0.3$; only one has a redshift higher than 0.5. Finally, the inset to Figure 5 shows the redshift measurements corresponding to $v_r < 1000$ km s^{-1}. Again, we define those with $v_r < 500$ km s^{-1} to be Galactic, although several could arise from the Local Group or beyond.

5. RESULTS

5.1. The UVQS Sample of New UV-bright Quasars

The principal goal of the UVQ Survey is to generate a new sample of FUV-bright quasars at $z \sim 1$. This motivated our target color criteria and subsequent observing strategy. With over 1000 sources analyzed, we may reassess the survey design and efficacy. Figure 6 presents the UV and *WISE* colors of the AGN measured in UVQS DR1, which includes both the primary (FUV–NUV > 0.3 mag) and secondary ($-0.5 <$ FUV–NUV < 0.3) candidates. As the source redshifts increase from $z = 0.1$–2, their observed UV and near-IR colors redden. We expect that the UV trend is due primarily to Lyman limit opacity from intervening H I gas, although a flattening of the AGN SED at approximately 1000 Å could contribute (e.g., Telfer et al. 2002; Lusso et al. 2015). The evolution in *W*1–*W*2 color must be intrinsic, i.e., it is related to the *k*-correction, which shifts from the rest-frame near-IR toward the optical with increasing AGN

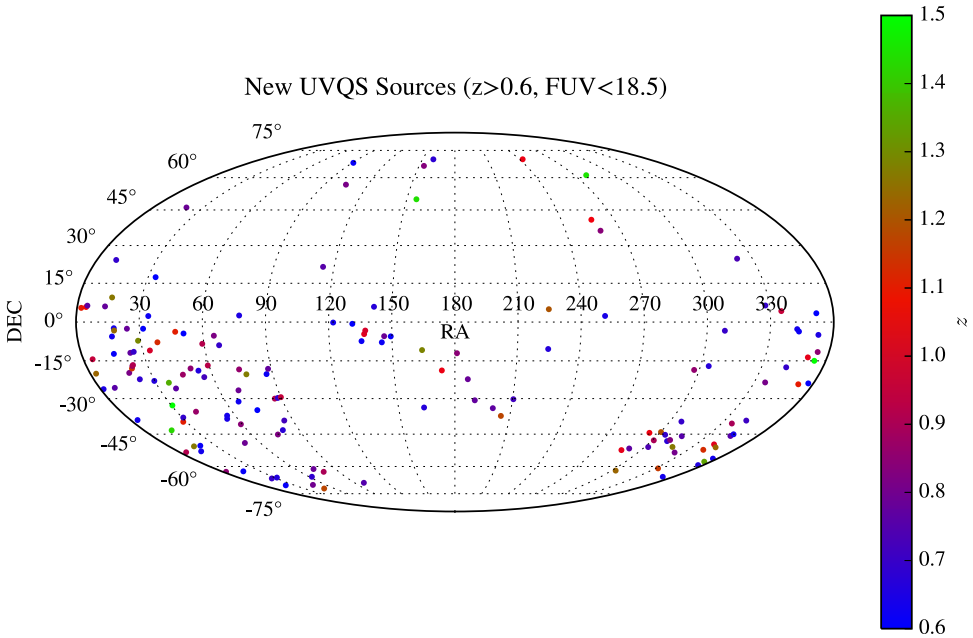

Figure 8. All-sky distribution of the new FUV-bright AGNs at $z > 0.6$, spectroscopically confirmed in our UVQS DR1 survey. The majority of these lie toward the Southern Galactic Pole.

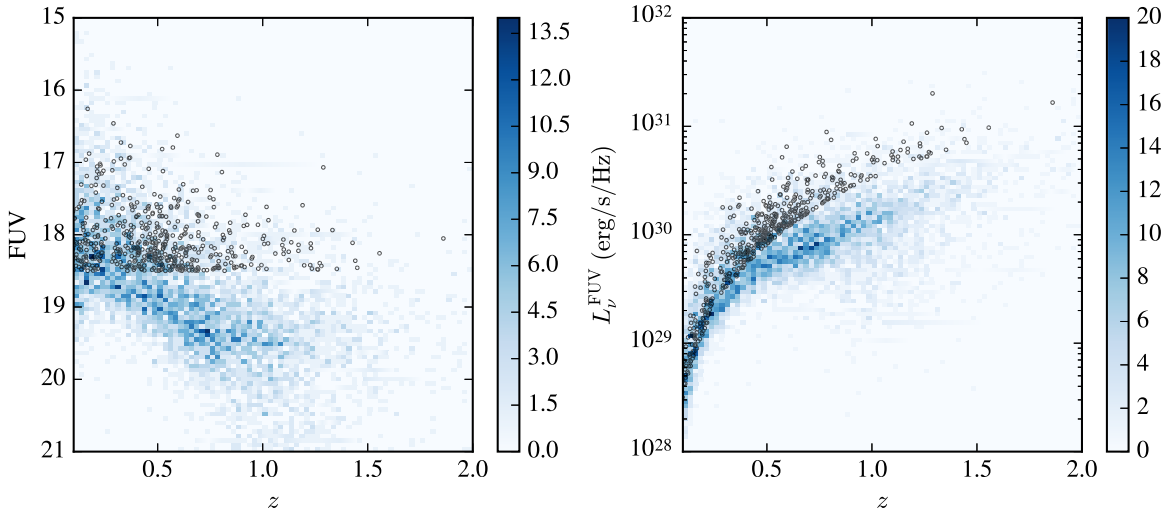

Figure 9. (Left) FUV *GALEX* magnitudes for the AGNs in the UVQS DR1 (black dots) compared against the locus of magnitudes from all previously known AGNs (blue, 2D histogram). The sources with FUV < 18 mag would yield good quality COS spectra in a modest orbit allocation. (Right) Specific FUV luminosities with the same symbol and color coding. At $z > 0.5$, the UVQS sources represent the most UV luminous AGNs on the sky.

redshift (e.g., Assef et al. 2010; Stern et al. 2012). In hindsight, we recognize that one could more efficiently target $z \sim 1$ quasars by adjusting the $W1 - W2$ cut to a larger value (e.g., 1.1 mag).

The efficacy of our survey can be assessed in terms of the fraction of AGNs recovered from the total number of sources observed. These results are presented in Figure 7, restricting to the primary candidates. Of 1040 primary candidates observed, we recovered a secure redshift for an extragalactic AGN for 86% of the objects. The remainder are split rather evenly between Galactic sources, poor spectra, and sources without an evident spectral feature. These are discussed further in the following sections.

Restricting to the $z > 0.6$ quasars from UVQS DR1 that were not listed in the v4.5 of the MILLIQUAS catalog, Figure 8 shows the sky distribution of these new sources. As expected, the majority of the new discoveries occur outside of the SDSS footprint, i.e., toward the Southern Galactic pole. Inspecting several of the sources within the SDSS footprint, we find they have good photometry and presume they were simply not targeted due to fiber collisions.

In Figure 9, we compare the FUV magnitudes and estimated luminosities (without corrections for Galactic extinction) of the new UVQS DR1 AGNs. These are compared against previously known sources; specifically, we show a 2D histogram of all sources from the MILLIQUAS catalog lying within 5 arcsec[10] of an FUV-detected source in the GALEXGR6Plus7 photoobjall catalog. At $z > 0.5$, the UVQS

[10] We caution that a small set of these previously cataloged quasars may have erroneous redshifts (see Section 4 for an example) or are a chance coincidence match to the *GALEX* catalog.

Table 4
UVQ DR1 AGNs

Name	z	$\sigma(z)$[a]	Z_QUAL[b]	New?[c]
UVQSJ000000.15-200427.7	0.291	0.003	4	Y
UVQSJ000503.70-391747.9	0.652	0.003	3	N
UVQSJ000609.57-261140.5	0.648	0.003	3	Y
UVQSJ000741.00-635145.8	0.559	0.003	3	N
UVQSJ000750.78+031733.1	1.101	0.003	4	N
UVQSJ000755.67+052818.8	1.098	0.003	4	Y
UVQSJ000856.77-235317.5	0.844	0.003	3	N
UVQSJ001015.62-624045.1	0.850	0.003	3	Y
UVQSJ001121.73-200212.1	1.226	0.003	4	Y
UVQSJ001155.60-240438.8	0.767	0.003	3	N
UVQSJ001521.62-385419.1	0.633	0.003	3	Y
UVQSJ001637.90-054424.8	0.074	0.003	5	Y
UVQSJ001641.88-312656.6	0.360	0.003	5	N
UVQSJ001653.66-530932.6	0.914	0.003	3	Y
UVQSJ001655.68+054822.9	1.060	0.003	3	Y
UVQSJ001705.14-312536.4	0.838	0.003	3	N
UVQSJ001753.32-142310.9	0.945	0.003	3	Y
UVQSJ001859.75+061931.9	0.767	0.003	3	Y
UVQSJ001903.85+423809.0	0.113	0.003	5	Y
UVQSJ002049.31-253829.0	0.645	0.003	3	N
UVQSJ002051.30-190126.8	0.962	0.003	3	N

Notes.
[a] Redshift uncertainty was derived from a template fit to the spectrum. We report a minimum redshift error of 0.003 from systematic uncertainties.
[b] Redshift quality: 0—No constraint, 3—Confident, 5—Excellent.
[c] Source is greater than 10 arcsec offset any quasar in the MILLIQUAS catalog (v4.5) with a published spectroscopic redshift.

(This table is available in its entirety in machine-readable form.)

DR1 AGNs are among the brightest and most luminous FUV sources known. A follow-up analysis studying the Eddington ratio, host galaxies, and galactic environment of these extreme sources could be valuable. Given the high efficiency of our survey, we expect that the community has now identified nearly every FUV-bright quasar on the sky. The only exceptions will be within the areas not surveyed by *GALEX* and the few lucky sources that shine through the dust of the Galactic plane.

One of the most luminous quasars from our survey, UVQSJ015454.68–071222.2 ($z = 1.289$, FUV $= 17.07$ mag; Figure 3), has an interesting history that is worth relating. This source was cataloged in 1962 by Haro & Luyten as PHL 1228 (Haro & Luyten 1962). Based on its color and coordinates, those authors identified the source as a candidate faint blue halo star toward the South Galactic pole. Indeed, a number of their candidates have since been confirmed as extragalactic AGNs. Clearly, a systematic redshift survey of the complete PHL catalog is warranted.

5.2. Other Sources

Figure 10 shows an all-sky plot of the other UVQS sources: AGNs at $z < 0.6$, sources with good spectra but without a precise redshift, and Galactic sources. Not surprisingly, the latter are primarily located near the Galactic plane. In DR1, we observed 66 sources satisfying our color criteria (including 24 with FUV–NUV < 0.3 mag) whose spectra yield a recessional velocity $v_r < 500$ km s^{-1}. These are listed in Table 5. Spectra for a representative set are shown in Figure 11. These objects include hot stars, white dwarfs, planetary nebulae, and Herbig Ae/Be stars, all of which have high surface temperatures explaining their high UV fluxes. It is more difficult, however, to explain their $W1 - W2$ colors. Several of the sources have *WISE* fluxes near their detection limit, i.e., poor photometry may explain their inclusion. Another set has substantial extinction ($E(B - V) > 0.3$ mag). The remainder, however, may be chance superpositions with a low-mass star. Finally, we note that from the full set of Galactic sources we identify a small sample with highly unusual spectra (e.g., Margon et al. 2016).

There are 93 sources with a good quality spectrum (SPEC_QUAL $\geqslant 3$) for which we cannot recover a secure redshift. The majority of these have been previously cataloged as blazars (or BL Lac objects). Examining Figure 10, we note these sources are distributed across the sky, consistent with an extragalactic origin. Table 6 lists the sample of these unknowns.

Finally, 48 of the brightest primary candidates (FUV < 17.5 mag) went unobserved. Nearly all of these are well resolved in the SDSS or DSS imaging and were dismissed as having

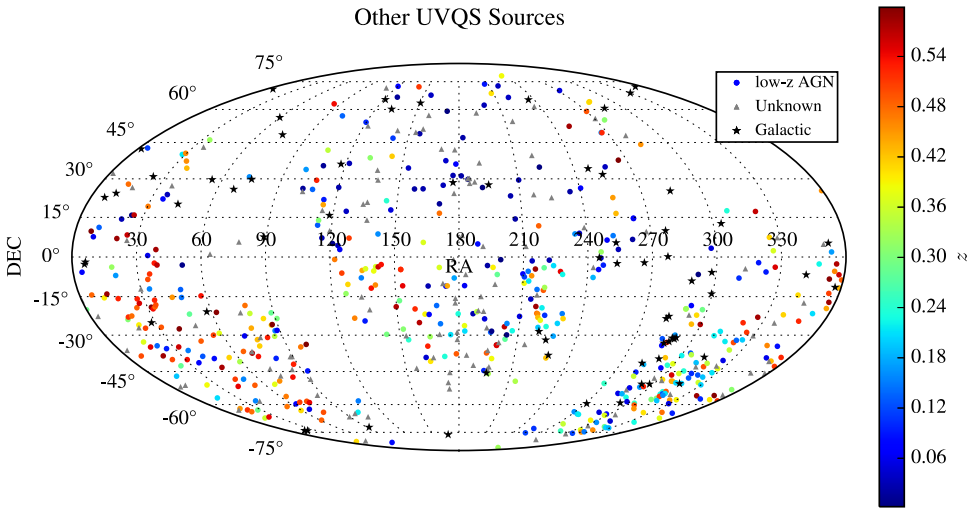

Figure 10. All-sky distribution of sources other than $z > 0.6$ AGNs drawn from our UVQS DR1 data set.

Table 5
UVQ DR1 Galactic Sources

Name	l (°)	b (°)	W_1 (mag)	W_2 (mag)	$E(B-V)$ (mag)
UVQSJ000717.69+421646.6	114.2718	−19.8486	12.44	11.51	0.07
UVQSJ002255.11−024418.7	106.0850	−64.6733	13.25	12.12	0.03
UVQSJ002324.11+704009.9	120.5946	7.9250	7.28	6.58	0.95
UVQSJ002452.54−015335.4	107.6594	−63.9745	9.56	8.69	0.03
UVQSJ002715.37+224158.1	115.6634	−39.8307	13.15	11.96	0.04
UVQSJ004433.61+241919.7	120.9291	−38.5229	11.41	10.81	0.05
UVQSJ011219.70−735126.0	300.9427	−43.1902	9.66	8.52	0.04
UVQSJ012138.72−735841.0	300.0898	−42.9831	9.98	9.31	0.05
UVQSJ013450.10+305445.0	133.7961	−31.0421	14.86	13.79	0.05
UVQSJ015159.68−250314.9	207.6540	−76.2551	17.82	16.34	0.01
UVQSJ025637.57+200537.2	158.9238	−33.8856	7.84	7.22	1.24
UVQSJ033900.56+294145.6	161.1830	−20.4629	7.61	6.83	0.22
UVQSJ035056.00−204815.9	214.1511	−48.7234	9.66	9.02	0.07
UVQSJ035859.45+561112.5	146.9221	2.3142	5.43	4.36	0.96
UVQSJ043243.03+255230.8	172.8867	−14.8704	6.25	5.48	1.37
UVQSJ045640.88+482057.8	158.6602	3.2547	8.55	7.84	0.65
UVQSJ045846.26+295036.7	173.4658	−7.9023	4.87	3.93	0.54
UVQSJ055504.39+073650.6	199.5921	−8.8793	11.93	11.21	0.59
UVQSJ060819.93−715737.4	282.5738	−29.0191	13.15	11.11	0.09
UVQSJ074955.94+355630.0	184.2155	26.7155	14.47	13.22	0.05
UVQSJ075320.02+154647.6	205.2586	20.6404	10.04	9.04	0.03
UVQSJ080430.46+645952.8	151.2065	32.0840	8.93	7.84	0.05
UVQSJ084551.18+600914.1	156.3057	37.4128	17.17	16.43	0.08
UVQSJ100201.71+631122.0	148.2491	44.7185	14.69	14.02	0.02
UVQSJ110923.71−762320.9	296.9168	−14.7238	7.23	6.47	0.68
UVQSJ114758.55+283156.2	203.5315	75.9099	16.31	15.60	0.02
UVQSJ125927.77+273810.5	49.3078	88.1476	13.89	13.09	0.01
UVQSJ130340.80−453722.7	305.1720	17.1955	14.82	13.78	0.09
UVQSJ144109.61−283020.9	330.3496	28.4600	16.15	15.48	0.10
UVQSJ145840.40−315439.7	332.1683	23.6398	16.26	15.63	0.14
UVQSJ151250.86−380731.6	331.3257	16.8283	10.86	9.68	0.11
UVQSJ154144.91+645352.3	99.5381	43.7046	14.68	13.86	0.03
UVQSJ162104.41−001610.7	13.3195	32.7354	12.76	11.95	0.11
UVQSJ162954.57+340706.0	55.5065	43.0309	17.65	16.32	0.02
UVQSJ165308.43+052323.2	23.7178	28.6949	15.54	14.48	0.12
UVQSJ165427.11−022700.4	16.2867	24.5149	12.85	11.87	0.28
UVQSJ165528.14+314556.5	53.6062	37.3588	17.07	16.22	0.03
UVQSJ174506.57−020844.1	23.2521	13.6944	11.08	10.04	0.41
UVQSJ180338.08−593009.5	334.2886	−17.4199	16.38	15.76	0.11
UVQSJ182754.20+095854.6	39.2363	9.7232	8.68	7.93	0.18
UVQSJ182847.85+000839.8	30.4732	5.1018	5.18	4.14	2.75
UVQSJ184635.12−232648.2	11.3414	−9.4477	10.20	9.39	0.43
UVQSJ184722.00−412632.5	354.4815	−16.8549	13.24	12.17	0.07
UVQSJ185026.03−223422.9	12.5279	−9.8712	11.81	10.89	0.40
UVQSJ185807.27+251417.3	56.3445	9.8431	15.19	14.44	0.28
UVQSJ190319.80+603553.6	91.0096	21.9990	14.24	13.56	0.05
UVQSJ190535.95−331138.0	3.8947	−17.1953	13.09	12.23	0.10
UVQSJ191423.34−323416.9	5.2059	−18.6908	14.58	13.65	0.10
UVQSJ191628.22−090236.7	27.6472	−9.6415	11.07	10.18	0.31
UVQSJ191652.27−310717.3	6.8342	−18.6662	13.17	12.34	0.09
UVQSJ191723.48−393646.8	358.3460	−21.6053	10.25	9.52	0.12
UVQSJ192210.62−313038.8	6.8718	−19.8639	13.44	12.54	0.11
UVQSJ192420.60−305822.8	7.5794	−20.1116	14.66	13.89	0.08
UVQSJ193037.67−502817.4	347.4837	−26.6214	16.17	15.49	0.06
UVQSJ193625.31−591135.8	337.8759	−28.7204	17.13	16.43	0.09
UVQSJ195006.99−502846.6	348.0512	−29.6809	16.49	15.56	0.04
UVQSJ195151.72−054816.6	34.6144	−16.0731	4.71	3.82	0.16
UVQSJ195838.50−135653.9	27.6059	−21.0742	6.58	5.96	0.33
UVQSJ201508.85+124215.2	54.1969	−12.1123	9.99	9.08	0.18
UVQSJ205321.33−385543.6	3.4324	−39.6203	14.81	13.77	0.05
UVQSJ210229.90−501631.7	348.5034	−41.1883	15.70	15.01	0.04
UVQSJ220030.64+682822.8	108.2571	10.6202	7.39	6.53	0.33
UVQSJ224840.11−064246.4	62.3103	−54.4269	16.75	16.11	0.04

Table 5
(Continued)

Name	l (°)	b (°)	W_1 (mag)	W_2 (mag)	$E(B-V)$ (mag)
UVQSJ232847.35+051451.4	88.1689	−51.9569	11.52	10.72	0.07
UVQSJ233145.86+720122.5	116.8008	10.1061	16.28	15.29	0.53
UVQSJ234823.76−112802.1	76.4925	−68.4481	16.64	15.86	0.03

Note. UVQS DR1 sources with recessional velocity $v_r < 500$ km s^{-1}. Reddening $E(B-V)$ estimates are based on the Schlegel et al. (1998) extinction maps.

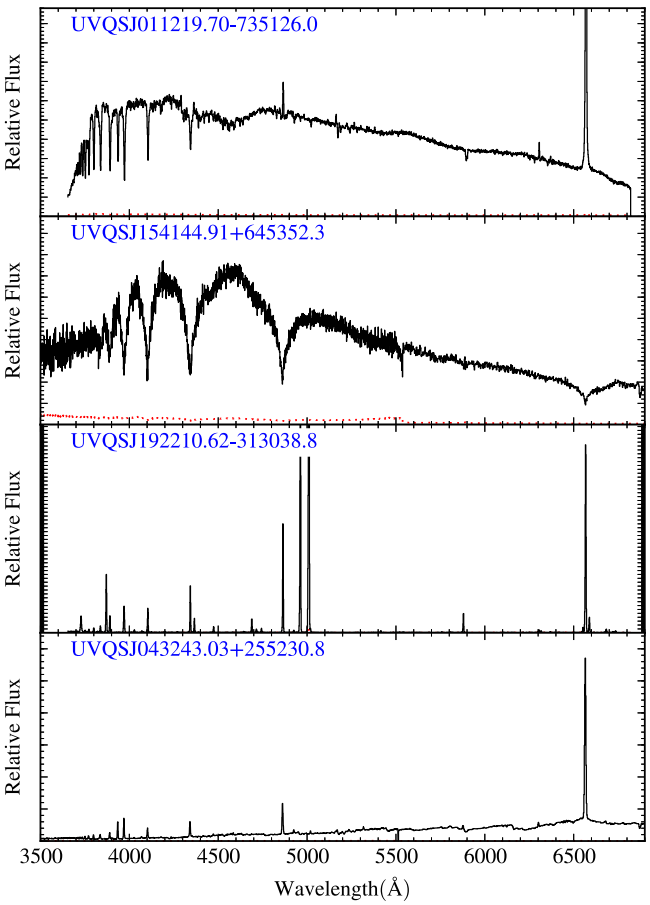

Figure 11. UVQS DR1 spectra for a representative set of Galactic sources unintentionally observed in our survey. The red dotted lines show an estimate of the 1σ uncertainties.

$z \ll 1$. Three of the sources–J124735.07-035008.2, J221153.89+184149.9, J221712.27+141420.9—went unobserved due to errors in bookkeeping or insufficient observing time. We will endeavor to provide spectra of these sources in our second data release.

6. CONCLUDING REMARKS

We have performed an all-sky survey for $z \sim 1$, FUV-bright quasars selected from *GALEX* and *WISE* photometry. The majority of these candidates lie toward the Southern Galactic Pole, i.e., outside the SDSS footprint. We confirmed 256 AGNs at $z > 0.6$, 155 of which had no previously reported spectroscopic redshift. Altogether, the UVQS DR1 includes 217 previously uncataloged AGNs with FUV < 18 mag, which are excellent targets for absorption-line analysis using *HST*/COS. Indeed, a handful of these AGNs are already scheduled for Cycle 24 observations. In our second data release of UVQS, we expand the search to NUV-bright AGNs at $z \sim 1$.

We kindly thank Kate Rubin and Neil Crighton for their twilight observations of several candidates. T.R.M. and J.T. acknowledge support for this project from the STScI Director's Discretionary Research Fund under allocation D0001.82451. J.X.P. and N.T. acknowledge partial support from the National Science Foundation (NSF) grant AST-1412981. J.F.H. acknowledges generous support from the Alexander von Humboldt Foundation in the context of the Sofja Kovalevskaja Award. The Humboldt Foundation is funded by the German Federal Ministry for Education and Research.

This work is based on data obtained from Lick Observatory, owned and operated by the University of California. We thank the Mount Hamilton staff of Lick Observatory for assistance in acquiring the observations.

This publication makes use of observations collected at the Centro Astronómico Hispano Alemán (CAHA) at Calar Alto, operated jointly by the Max-Planck Institut fur Astronomie and the Instituto de Astrofísica de Andalucía (CSIC).

Some of the data presented herein were obtained at the W.M. Keck Observatory, which is operated as a scientific partnership among the California Institute of Technology, the University of California, and the National Aeronautics and Space Administration. The Observatory was made possible by the generous financial support of the W.M. Keck Foundation. Some of the Keck data were obtained through the NSF Telescope System Instrumentation Program (TSIP), supported by AURA through the NSF under AURA Cooperative Agreement AST 01-32798 as amended. The authors wish to recognize and acknowledge the very significant cultural role and reverence that the summit of Mauna Kea has always had within the indigenous Hawaiian community. We are most fortunate to have the opportunity to conduct observations from this mountain.

This publication makes use of data products from the *Wide-field Infrared Survey Explorer*, which is a joint project of the University of California, Los Angeles, and the Jet Propulsion Laboratory/California Institute of Technology, and *NEOWISE*, which is a project of the Jet Propulsion Laboratory/California Institute of Technology. *WISE* and *NEOWISE* are funded by the National Aeronautics and Space Administration.

Table 6
UVQ DR1 Unknown Sources

Name	l (°)	b (°)	FUV (mag)	NUV (mag)
UVQSJ000009.65−163441.4	71.9317	−74.1194	18.48	17.72
UVQSJ001444.02−223522.6	59.5364	−80.5220	18.39	17.34
UVQSJ001529.53−360535.3	341.1397	−78.2250	18.23	17.70
UVQSJ004038.09−505756.5	307.1282	−66.0744	17.43	16.77
UVQSJ005116.64−624204.3	302.9636	−54.4270	18.31	17.84
UVQSJ010018.69−741815.9	302.1140	−42.8097	17.55	17.12
UVQSJ012031.66−270124.6	213.6632	−83.5246	18.20	17.36
UVQSJ013955.76+061922.4	144.0255	−54.5508	17.64	17.19
UVQSJ022239.60+430207.8	140.1429	−16.7669	17.70	16.88
UVQSJ024440.30−581954.5	278.4481	−53.0779	18.48	18.09
UVQSJ024553.03−803533.7	297.4299	−35.2790	18.43	17.29
UVQSJ041652.49+010523.8	191.8145	−33.1591	18.06	17.71
UVQSJ044924.69−435008.9	248.8052	−39.9188	15.89	15.34
UVQSJ045953.82−464958.1	252.6989	−38.1225	18.38	18.03
UVQSJ050925.96+054135.3	195.4054	−19.6361	18.47	17.48
UVQSJ051354.64−305318.5	233.6318	−33.3244	18.07	17.72
UVQSJ053850.36−440508.9	250.0828	−31.0896	17.96	16.58
UVQSJ054357.22−553207.3	263.5150	−31.4742	18.12	17.74
UVQSJ055417.57−383951.1	244.6776	−27.1526	15.86	14.58
UVQSJ055942.72−660908.1	275.9131	−29.8399	18.27	17.71
UVQSJ063146.38−642615.1	274.2555	−26.3760	17.17	16.65
UVQSJ065046.48+250259.5	190.2825	10.9956	18.08	17.44
UVQSJ070031.25−661045.2	276.7686	−23.7595	18.11	17.45
UVQSJ072153.46+712036.3	143.9811	28.0176	15.40	14.67
UVQSJ073807.39+174219.0	201.8465	18.0706	18.48	17.33
UVQSJ080949.18+521858.2	166.2451	32.9104	17.16	16.71
UVQSJ085448.87+200630.6	206.8121	35.8209	18.27	17.42
UVQSJ085500.56−150523.7	241.8511	18.8133	18.38	17.62
UVQSJ090226.91+205046.5	206.6753	37.7519	18.42	17.80
UVQSJ090534.98+135806.4	215.0300	35.9597	17.85	17.25
UVQSJ091037.03+332924.4	191.1205	42.4663	17.17	16.44
UVQSJ091552.39+293323.9	196.6498	42.9348	17.44	16.83
UVQSJ101234.19−301226.7	266.6004	21.2358	16.58	16.72
UVQSJ101504.13+492600.7	165.5339	52.7122	16.72	16.27
UVQSJ102356.17−433601.5	276.5969	11.6016	18.03	17.30
UVQSJ103744.29+571155.5	151.7712	51.7826	18.43	17.69
UVQSJ110436.60−390352.8	281.2378	19.2650	16.69	16.88
UVQSJ112048.05+421212.5	167.8538	66.1628	18.18	17.66
UVQSJ113405.66−494455.5	290.3338	11.2217	16.65	16.91
UVQSJ113601.74−523515.8	291.4799	8.5992	17.22	17.69
UVQSJ113858.26−452304.3	289.8239	15.6348	15.85	16.11
UVQSJ114946.72−005456.6	272.5734	58.2743	17.23	17.65
UVQSJ115034.76+415440.0	159.1108	70.6800	18.33	17.69
UVQSJ115255.65−172239.3	283.5971	43.2867	18.45	17.96
UVQSJ115315.22−153637.1	282.9313	44.9899	17.28	16.52
UVQSJ115628.86−284431.8	288.6213	32.5978	15.88	16.29
UVQSJ115643.52−313925.4	289.5217	29.7860	17.35	17.19
UVQSJ121241.46−063309.9	285.9713	55.0380	17.28	16.92
UVQSJ121623.79−380242.8	295.3691	24.3114	17.49	17.32
UVQSJ121752.08+300700.6	188.8749	82.0529	16.65	16.05
UVQSJ122121.94+301037.1	186.3587	82.7345	16.75	16.29
UVQSJ122131.68+281358.4	201.7355	83.2880	17.16	16.48
UVQSJ123212.01−421750.5	299.1374	20.4326	16.77	16.83
UVQSJ123730.73−201829.0	298.5057	42.4440	18.05	17.20
UVQSJ124312.73+362743.9	133.0071	80.5046	17.12	16.37
UVQSJ125535.09−270230.8	304.0707	35.8207	16.66	16.88
UVQSJ130059.12−360619.8	305.0909	26.7262	18.28	17.31
UVQSJ130421.00−435310.2	305.3908	18.9239	17.50	16.83
UVQSJ130737.98−425938.9	306.0779	19.7787	17.56	16.85
UVQSJ130748.03−101758.5	309.5316	52.3624	16.63	16.72
UVQSJ132225.65−325431.5	310.4044	29.5130	17.95	16.25
UVQSJ140450.90+040202.2	343.3271	61.0101	17.44	17.08
UVQSJ141649.18−334117.3	322.6069	25.9006	17.44	17.34

Table 6
(Continued)

Name	l (°)	b (°)	FUV (mag)	NUV (mag)
UVQSJ141946.61+542314.8	98.3006	58.3118	17.71	16.75
UVQSJ142700.39+234800.0	29.4873	68.2076	16.26	15.66
UVQSJ143917.46+393242.8	68.8479	64.4232	17.83	17.26
UVQSJ150101.86+223806.3	31.4457	60.3502	17.35	16.69
UVQSJ154256.97+612955.0	95.3924	45.3923	17.92	17.11
UVQSJ155543.17+111124.6	21.9093	43.9637	16.08	15.38
UVQSJ161020.67−035506.1	7.9353	32.8755	18.49	18.31
UVQSJ175132.81+093900.7	34.9194	17.6452	18.39	17.32
UVQSJ180314.75+554245.0	83.9878	28.7766	18.32	17.43
UVQSJ183849.18+480234.4	76.9498	21.8288	17.80	17.21
UVQSJ190748.98−530021.4	343.8994	−23.7303	18.49	18.20
UVQSJ190926.48−793848.1	314.5806	−27.4588	15.78	15.99
UVQSJ192833.35−220353.7	16.7052	−17.7157	16.39	16.69
UVQSJ200549.12−754848.0	318.6171	−30.7726	18.28	18.13
UVQSJ200925.39−484953.6	350.3731	−32.6008	15.52	15.13
UVQSJ202053.28−650159.8	330.9495	−33.8002	18.16	17.97
UVQSJ205349.78−042429.8	43.6864	−29.1253	18.34	18.10
UVQSJ213924.16−423520.3	358.3175	−48.3262	17.22	16.61
UVQSJ215459.97+071949.8	65.3423	−35.1428	17.98	17.66
UVQSJ215852.06−301332.0	17.7305	−52.2458	13.87	13.48
UVQSJ222358.40−251043.5	27.8277	−56.9682	16.69	16.20
UVQSJ230029.52−172411.0	47.9236	−62.6290	18.23	17.78
UVQSJ231731.98−453359.6	342.0701	−63.7783	18.43	17.85
UVQSJ232444.66−404049.4	350.1952	−67.5844	17.29	16.82
UVQSJ233913.22−552350.8	322.8252	−58.8535	17.83	16.40
UVQSJ235123.69−454336.0	331.6648	−67.9074	18.50	18.09

Note. UVQS DR1 sources with good spectral quality but where no precise redshift could be measured.

Facilities: Shane (Kast Double spectrograph), Du Pont (Boller & Chivens spectrograph), CAO:2.2m (Calar Alto Faint Object Spectrograph), Keck:II (Echellette Spectrograph and Imager), MMT (MMT Blue Channel), Magellan:Clay (Magellan Echellette).

REFERENCES

Assef, R. J., Kochanek, C. S., Brodwin, M., et al. 2010, ApJ, 713, 970
Bianchi, L., Conti, A., & Shiao, B. 2014, AdSpR, 53, 900
Flesch, E. W. 2015, PASA, 32, 10
Haro, G., & Luyten, W. J. 1962, BOTT, 3, 37
Lehner, N., Howk, J. C., Tripp, T. M., et al. 2013, ApJ, 770, 138
Lehner, N., Savage, B. D., Richter, P., et al. 2007, ApJ, 658, 680
Lusso, E., Worseck, G., Hennawi, J. F., et al. 2015, MNRAS, 449, 4204
Margon, B., Prochaska, J. X., Tejos, N., & Monroe, T. 2016, PASP, 128, 024201
Meiring, J. D., Tripp, T. M., Werk, J. K., et al. 2013, ApJ, 767, 49
Pâris, I., Petitjean, P., Aubourg, É, et al. 2014, A&A, 563, A54
Richards, G. T., Vanden Berk, D. E., Reichard, T. A., et al. 2002, AJ, 124, 1
Schlegel, D. J., Finkbeiner, D. P., & Davis, M. 1998, ApJ, 500, 525
Schneider, D. P., Richards, G. T., Hall, P. B., et al. 2010, AJ, 139, 2360
Stern, D., Assef, R. J., Benford, D. J., et al. 2012, ApJ, 753, 30
Tejos, N., Morris, S. L., Finn, C. W., et al. 2014, MNRAS, 437, 2017
Tejos, N., Prochaska, J. X., Crighton, N. H. M., et al. 2016, MNRAS, 455, 2662
Telfer, R. C., Zheng, W., Kriss, G. A., & Davidsen, A. F. 2002, ApJ, 565, 773
Tripp, T. M., Meiring, J. D., Prochaska, J. X., et al. 2011, Sci, 334, 952
Tripp, T. M., Sembach, K. R., Bowen, D. V., et al. 2008, ApJS, 177, 39
Tumlinson, J., Thom, C., Werk, J. K., et al. 2013, ApJ, 777, 59
Werk, J. K., Prochaska, J. X., Thom, C., et al. 2013, ApJS, 204, 17
Werk, J. K., Prochaska, J. X., Tumlinson, J., et al. 2014, ApJ, 792, 8